White Noise Array Gain for Minimum Variance Distortionless Response Beamforming With Fractional Lower Order Covariance

AIMIN SONG

School of Science, Dalian Jiaotong University, Dalian 116028, China

e-mail: songaimin@djtu.edu.cn

ABSTRACT In this paper, a special property of the fractional lower order covariance (FLOC)-based minimum variance distortionless response (MVDR) beamformer is found, which is the FLOC MVDR beamformer that has greater white noise array gain (WNAG) than the classic MVDR beamformer in the presence of non-Gaussian stable noise. In order to explain the reason, the analytic WNAG of the FLOC MVDR beamformer is derived with respect to eigenvalues of FLOC matrix. Then, it is theoretically proved and explained through the relation between the WNAG and the eigenvalue separation of the covariance matrix and the reason can be concluded that the eigenvalue separation of the FLOC-based matrix is weaker than that of conventional covariance. Simulation results verify the validity and advantages of the FLOC MVDR beamformer over the MVDR beamformer when the received array noise obeys stable distributions and there exist steering vector mismatches in the beamforming model.

INDEX TERMS Beamforming, fractional lower order covariance, stable distributions, white noise array gain.

I. INTRODUCTION

Adaptive beamforming enhances the signal of interest (SOI) and suppresses the interference and the noise at the outputs of an antenna array. Therefore, it has been widely adopted in many applications including radar [1], [2], wireless communication [3] and wireless sensor network [4], [5]. Among the approaches proposed in the field of the beamforming techniques, minimum variance distortionless response (MVDR) beamforming is a popular and practical one. Subjecting to the linear constraint, MVDR beamforming selects the weight vector and minimizes the output power adaptively, which causes no distortion to the SOI [1].

Conventional MVDR beamforming assumes the additive noise is Gaussian distributed. In many practical situations, however, the noise is more impulsive and cannot be considered as Gaussian noise [6]. Recent studies show that alpha-stable distribution is an ideal option to model this kind of non-Gaussian noise [6]–[11] and it is termed as the fractional lower-order alpha-stable (FLOA) distribution when its characteristic exponent $\alpha < 2$ [6]. The probability density function of FLOA is heavy-tailed and α

controls the impulsiveness. In particular, alpha-stable distributions can be applied to depict Gaussian distributions when $\alpha = 2$.

There are numerous literatures on robust beamforming methods in the presence of alpha-stable noise. For example, Tsakalides and Nikias [12] address a robust beamforming technique based on the fractional lower-order moment theory and this method exhibits resistance to the presence of alpha-stable noise. To suppress the adverse effect of the impulsive noise, FLOC is utilized to force the nulls closer to the DOA of interference in [13] and [14]. Subjecting to linear constraints, geometric power is employed as the cost function in [15] to propose robust beamforming for the heavy-tailed stable noise. In [16], the infinite-norm is used to normalize the received data and this approach offers better interference rejection ability. For a generalized constant modulus beamforming, the convergence [17] and capture properties [18] are presented in the presence of alpha-stable noise, respectively. In [19], a robust M-estimation orthonormal PAST beamforming is proposed to combat the hostile effect of impulsive stable noise.

The purpose of this paper is to explain the property that the WNAG of the FLOC MVDR beamformer is greater than that of the conventional MVDR beamformer under the FLOA noise, which is found by simulation. WNAG is an evaluation parameter of the robustness for beamforming methods [1]. To the best of our knowledge, there is little attention on the WNAG of the beamforming in the presence of the FLOA noise. To clarify the occurrence of this phenomenon, the WNAG of the FLOC MVDR beamformer in the presence of the FLOA noise is studied and its explicit expression is addressed as well. With the help of this expression, we analyze the relationship between the WNAG and the eigenvalue separation of the covariance matrix.

The remaining of the paper is organized as follows. The MVDR beamformer and the FLOC MVDR beamformer are introduced in Section II. Section III contains our main work which explains why the FLOC MVDR beamformer has greater WNAG than the conventional MVDR beamformer in the presence of the FLOA noise. Furthermore, we discuss the similarities between the diagonal loading (DL) MVDR beamformer and the FLOC MVDR beamformer in Section IV. Section V involves the simulation results of the FLOC MVDR beamformer when the received array noise obeys stable distributions. Finally, conclusions are drawn in Section VI.

The following notations are used throughout the paper. The superscripts $(\cdot)^*$, $(\cdot)^T$, $(\cdot)^H$ and $(\cdot)^{-1}$ stand for conjugate, transpose, conjugate transpose and matrix inverse, respectively. $\mathbb{E}[\cdot]$ is the mathematical expectation. $\|\cdot\|$ stands for the Euclidean norm. $\Re[\cdot]$ denotes the real part of a complex.

II. MVDR BEAMFORMING AND FLOC MVDR BEAMFORMING

In this section, we introduce the fundamental framework of beamforming including the beamforming model, the MVDR beamformer and the FLOC MVDR beamformer.

A. BEAMFORMING MODEL

Consider a uniform linear array (ULA) with M omnidirectional sensors and an adjacent sensor spacing d. Suppose that there are $J + 1$ $(J + 1 \leq M)$ narrowband signals with wavelength λ impinging upon the arrays from the far field with DOA angles $\theta_0, \theta_1, \cdots, \theta_J$. Then the k-th snapshot vector $\mathbf{x}(k)$ of the received array signals can be expressed as

$$\mathbf{x}(k) = s_0(k)\mathbf{a}(\theta_0) + \sum_{j=1}^{J} s_j(k)\mathbf{a}(\theta_j) + \mathbf{v}(k),$$
$$k = 1, 2, \cdots, N, \quad (1)$$

where $s_0(k)$ and $s_j(k)$ $(j = 1, 2, \cdots, J)$ are the SOI and the j-th interference, respectively. Here, N is the number of training snapshots. The M-dimensional vector $\mathbf{a}(\theta_j)$ is the steer vector of $s_j(k)$ and $\mathbf{v}(k)$ is the additional noise vector

at instant k. Set $\beta_j = \frac{2\pi}{\lambda} d \sin(\theta_j)$. Then (1) can be written as

$$\begin{pmatrix} x_1(k) \\ x_2(k) \\ \vdots \\ x_M(k) \end{pmatrix} = \begin{pmatrix} 1 & 1 & \cdots & 1 \\ e^{j\beta_0} & e^{j\beta_1} & \cdots & e^{j\beta_J} \\ \vdots & \vdots & \ddots & \vdots \\ e^{j(M-1)\beta_0} & e^{j(M-1)\beta_1} & \cdots & e^{j(M-1)\beta_J} \end{pmatrix}$$
$$\cdot \begin{pmatrix} s_0(k) \\ s_1(k) \\ \vdots \\ s_J(k) \end{pmatrix} + \begin{pmatrix} v_1(k) \\ v_2(k) \\ \vdots \\ v_M(k) \end{pmatrix}, \quad (2)$$

where $v_i(k)$ is the i-th element of the vector $\mathbf{v}(k)$. Here we assume that $v_i(k)$ obeys an isotropic symmetric stable distribution.

A complex random variable $n = n_1 + in_2$ obeys an isotropic symmetric stable distribution if its characteristic function satisfies [6]

$$\mathbb{E}\left\{\exp\left(j\Re\left[\omega n^*\right]\right)\right\} = \exp\left(-\delta |\omega|^\alpha\right). \quad (3)$$

The parameter δ $(\delta > 0)$ denotes the dispersion, which plays a similar role to the variance of Gaussian distribution. The characteristic exponent α determines the shape of the distribution. More specifically, its tail becomes heavier as α decreases. In signal processing, the random variable n is Gaussian noise in the case of $\alpha = 2$ and n is called FLOA noise when $\alpha < 2$. We refer to [6] for more details about isotropic symmetric stable distributions.

Since the second order statistics do not converge in the presence of the FLOA noise [6], [11], [15], the conventional signal-to-noise ratio (SNR) and interference-to-noise ratio (INR) do not exist. Thus, the geometric power for the FLOA noise is established in [20] and [21] as an alternate of the conventional power. The geometric SNR is defined by [20]

$$\text{SNR}_G = 10 \log_{10} \left(\frac{\sigma_{s_0}^2}{\left(\sqrt{2C_g}u\right)^2} \right) \quad (4)$$

and the j-th geometric INR by

$$\text{INR}_G = 10 \log_{10} \left(\frac{\sigma_{s_j}^2}{\left(\sqrt{2C_g}u\right)^2} \right), \quad (5)$$

where the geometric power u is computed by

$$u = \frac{1}{M} \sum_{i=1}^{M} \exp\left(\mathbb{E}\left[\log_e |v_i|\right]\right); \quad (6)$$

the constant $C_g \approx 1.78$ is the exponential of Euler constant and $\sigma_{s_j}^2$ denotes the power of $s_j(k)(j = 0, 1, \cdots, J)$.

B. MVDR BEAMFORMING

The conventional MVDR beamforming, where the additive noise is assumed to be Gaussian distributed, is one of the classical approaches proposed in the beamforming techniques. In the Gaussian noise environment, the MVDR beamformer can be formulated as the following optimization problem :

$$\mathbf{w} = \arg \min \mathbf{w}^H \mathbf{R}_{i+n} \mathbf{w} \text{ s.t. } \mathbf{w}^H \mathbf{a}(\theta_0) = 1, \quad (7)$$

where

$$\mathbf{R}_{i+n} = \mathbb{E}\left\{\mathbf{x}_{i+n}(k)\mathbf{x}_{i+n}^H(k)\right\} \qquad (8)$$

is the covariance matrix of the interference plus noise

$$\mathbf{x}_{i+n}(k) = \sum_{j=1}^{J} s_j(k)\mathbf{a}\left(\theta_j\right) + \mathbf{v}(k). \qquad (9)$$

For convenience, we use the short-hand notation $\mathbf{a}_0 := \mathbf{a}\left(\theta_0\right)$. Through the Lagrange multiplier, the optimal solution of (7) is given by

$$\mathbf{w} = \mathbf{R}_{i+n}^{-1}\mathbf{a}_0\left(\mathbf{a}_0^H\mathbf{R}_{i+n}^{-1}\mathbf{a}_0\right)^{-1}. \qquad (10)$$

A major drawback of the conventional MVDR beamformer is the convergence incapability of $\mathbf{R}_{i+n}$ since the second statistics do not converge in the presence of the FLOA noise [6]. Therefore, the FLOC MVDR beamformer is established in [13] and [14] to remove the shortcoming.

C. FLOC MVDR BEAMFORMER
Compared with the conventional MVDR beamformer, the FLOC MVDR beamformer improves the robustness against the FLOA noise [13], [14]. Its weight is given by

$$\mathbf{w}_{\text{FLOC}} = \Gamma_{i+n}^{-1}\mathbf{a}_0\left(\mathbf{a}_0^H\Gamma_{i+n}^{-1}\mathbf{a}_0\right)^{-1}. \qquad (11)$$

Here the FLOC matrix of interference plus noise Γ_{i+n} is defined by

$$\Gamma_{i+n} = \mathbb{E}\left\{\tilde{\mathbf{x}}_{i+n}(k)\tilde{\mathbf{x}}_{i+n}^H(k)\right\}, \qquad (12)$$

where $\tilde{\mathbf{x}}(k)$ is of the following form:

$$\tilde{\mathbf{x}}(k) = \left[\tilde{x}_1(k), \tilde{x}_2(k), \cdots, \tilde{x}_M(k)\right]^T; \qquad (13)$$

$$\tilde{x}_i(k) = (x_i(k))^{\langle p \rangle}, \quad (\cdot)^{\langle p \rangle} = |\cdot|^{p-1}(\cdot)^* \qquad (14)$$

and p is the parameter we choose from the interval $(0, \frac{\alpha}{2})$. In [13] and [14], the convergence of Γ_{i+n} is proved in the presence of the FLOA noise when $0 < p < \frac{\alpha}{2}$. The FLOC matrix Γ_{i+n} reduces to the conventional covariance matrix $\mathbf{R}_{i+n}$ when the parameter $p = 1$ in (14). From this perspective, the FLOC MVDR beamformer in (11) can be regarded as the generalization of the MVDR beamformer in (10).

Note 1: Since the data $\mathbf{x}_{i+n}(k)$ in (9) is unknown in practice, it is substituted by the received array data $\mathbf{x}(k)$ [22]. Therefore, the beamformers (10) and (11) are usually obtained by

$$\mathbf{w} = \mathbf{R}_{\mathbf{x}}^{-1}\mathbf{a}_0\left(\mathbf{a}_0^H\mathbf{R}_{\mathbf{x}}^{-1}\mathbf{a}_0\right)^{-1} \qquad (15)$$

and

$$\mathbf{w}_{\text{FLOC}} = \Gamma_{\mathbf{x}}^{-1}\mathbf{a}_0\left(\mathbf{a}_0^H\Gamma_{\mathbf{x}}^{-1}\mathbf{a}_0\right)^{-1}, \qquad (16)$$

where

$$\mathbf{R}_{\mathbf{x}} = \mathbb{E}\left\{\mathbf{x}(k)\mathbf{x}^H(k)\right\} \qquad (17)$$

and

$$\Gamma_{\mathbf{x}} = \mathbb{E}\left\{\tilde{\mathbf{x}}(k)\tilde{\mathbf{x}}^H(k)\right\} \qquad (18)$$

are the covariance matrix and FLOC matrix of $\mathbf{x}(k)$, respectively.

III. WNAG DIFFERENCE BETWEEN FLOC MVDR BEAMFORMER AND CONVENTIONAL MVDR BEAMFORMER
WNAG is a significant measure of robustness for the MVDR beamformer against model uncertainties [1]. We find, by simulations, the WNAG of the FLOC MVDR beamformer is greater than that of the conventional MVDR beamformer under the FLOA noise. Why this phenomenon occurs is at the center of our interest. In this section, we clarify this issue from theoretical analysis. The corresponding simulations are implemented in V-A.

Given a beamforming weight vector $\mathbf{w}$, WNAG is defined by

$$G = \left(\|\mathbf{w}\|_2^2\right)^{-1}, \qquad (19)$$

where $\|\cdot\|_2$ is the 2-norm of vector. It has been proved in [1] that the sensitivity of the beamforming decreases with the increase of WNAG. Moreover, for a constant T_0, imposing a suitable constraint on the WNAG, i.e.,

$$\|\mathbf{w}\|_2^2 \leq T_0, \qquad (20)$$

results in robust beamforming against the array mismatches (e.g. [1], [22]). Furthermore, the constraint in (20) can be represented by the WNAG constraint (see [1]) as follows:

$$G = \left(\|\mathbf{w}\|_2^2\right)^{-1} \geq T_0^{-1}. \qquad (21)$$

In order to investigate the WNAG difference between the MVDR beamformer and the FLOC MVDR beamformer, we first define the covariance matrix Ω as

$$\Omega := \begin{cases} \Gamma_{\mathbf{x}} & \text{for FLOC MVDR beamformer} \\ \mathbf{R}_{\mathbf{x}} & \text{for MVDR beamformer.} \end{cases} \qquad (22)$$

Then we give the relationship between the WNAG and the eigenvalues of Ω in the following theorem, which is appropriate for both the FLOC MVDR beamformer and the conventional MVDR beamformer.

Theorem 1: Assume that the covariance matrix Ω in (22) is nonsingular. Then the WNAG of the MVDR beamformer G is given by

$$G = \frac{\left(t_1\lambda_1^{-1} + t_2\lambda_2^{-1} + \cdots + t_M\lambda_M^{-1}\right)^2}{t_1\lambda_1^{-2} + t_2\lambda_2^{-2} + \cdots + t_M\lambda_M^{-2}}, \qquad (23)$$

where $\lambda_1, \cdots, \lambda_M$ are the eigenvalues of Ω and the constant t_i, $i = 1, 2, \cdots, M$, satisfies $0 \leq t_i < M$ and $t_1 + t_2 + \cdots + t_M = M$.

Proof: See Appendix A.

Theorem 1 shows that the WNAG of the MVDR beamformer G is dominated by the eigenvalues of covariance

matrix Ω. However, it is virtually impossible to compare the eigenvalues of $\Gamma_{\mathbf{x}}$ with those of $\mathbf{R}_{\mathbf{x}}$ due to the nonlinearity of $\Gamma_{\mathbf{x}}$. This motivates us to study the relationship between the WNAG and the eigenvalue separation of Ω.

Definition 1: For the eigenvalues $\{\lambda_1, \lambda_2, \cdots, \lambda_M\}$ of Ω with $\lambda_1 \geq \lambda_2 \geq \cdots \geq \lambda_M > 0$, the eigenvalue separation Dis $(\lambda_1, \lambda_2, \cdots, \lambda_M)$ of Ω is defined by

$$\text{Dis}\,(\lambda_1, \lambda_2, \cdots, \lambda_M) := \frac{1}{M-1} \sum_{j=1}^{M-1} \frac{\lambda_M}{\lambda_j}. \quad (24)$$

Obviously, the less $\{\lambda_1, \lambda_2, \cdots, \lambda_M\}$ separates, the greater Dis $(\lambda_1, \lambda_2, \cdots, \lambda_M)$ becomes. Moreover, we have

$$0 < \text{Dis}\,(\lambda_1, \lambda_2, \cdots, \lambda_M) \leq 1 \quad (25)$$

and the eigenvalue separation attains the maximum value 1 if and only if $\lambda_1 = \lambda_2 = \cdots = \lambda_M$. Therefore, Dis $(\lambda_1, \lambda_2, \cdots, \lambda_M)$ can be regarded as a normalized measure of the separation for $\lambda_1 \geq \lambda_2 \geq \cdots \geq \lambda_M > 0$.

By multiplying λ_M^{-2} in both the numerator and the denominator of (23), the WNAG of the MVDR beamformer G can be written as

$$G = \frac{\left(t_1 \left(\frac{\lambda_M}{\lambda_1}\right) + t_2 \left(\frac{\lambda_M}{\lambda_2}\right) + \cdots + t_M\right)^2}{t_1 \left(\frac{\lambda_M}{\lambda_1}\right)^2 + t_2 \left(\frac{\lambda_M}{\lambda_2}\right)^2 + \cdots + t_M}. \quad (26)$$

Set

$$u_1 = \frac{\lambda_M}{\lambda_1}, \quad u_2 = \frac{\lambda_M}{\lambda_2}, \quad \cdots, \quad u_{M-1} = \frac{\lambda_M}{\lambda_{M-1}}. \quad (27)$$

Then (24) and (26) give rise to

$$\text{Dis}\,(\lambda_1, \lambda_2, \cdots, \lambda_M) = \frac{1}{M-1} \sum_{j=1}^{M-1} u_j \quad (28)$$

and

$$\begin{aligned} G : &= h\,(u_1, u_2, \cdots, u_{M-1}) \\ &= \frac{(t_1 u_1 + t_2 u_2 + \cdots + t_{M-1} u_{M-1} + t_M)^2}{t_1 u_1^2 + t_2 u_2^2 + \cdots + t_{M-1} u_{M-1}^2 + t_M}. \end{aligned} \quad (29)$$

Hence, both the eigenvalue separation of Ω and the WNAG of the MVDR beamformer G are the functions of $u_1, u_2, \cdots, u_{M-1}$. Next, we will study how u_i, $i \in \{1, 2, \ldots, M-1\}$, exerts impacts on the WNAG of the MVDR beamformer $G = h\,(u_1, u_2, \cdots, u_{M-1})$.

Theorem 2: Let $u_{M-1} \ll 1$. Then we have

$$\frac{\partial G}{\partial u_i} = \frac{\partial h\,(u_1, u_2, \cdots, u_{M-1})}{\partial u_i} > 0, \quad i = 1, 2, \cdots, M-1. \quad (30)$$

Proof: See Appendix B.

We see in Theorem 2 that the WNAG of the MVDR beamformer G is a monotone increasing function of each u_i, $i = 1, 2, \ldots, M-1$. In the case of $\alpha < 2$ and $p < 1$, the eigenvalue separation Dis $(\lambda_1, \lambda_2, \cdots, \lambda_M)$ of $\Gamma_{\mathbf{x}}$ in (18) is bigger than that of $\mathbf{R}_{\mathbf{x}}$ in (17). This means, u_i of $\Gamma_{\mathbf{x}}$ is larger

than that of $\mathbf{R}_{\mathbf{x}}$, which gives rise to the phenomenon that the FLOC MVDR beamformer, compared with the conventional MVDR beamformer, has greater WNAG.

Based on the above analysis, we conclude that the reason why the FLOC MVDR beamformer possesses greater WNAG than the conventional MVDR beamformer under the FLOA noise is that the eigenvalues of the FLOC matrix separate less than those of the conventional covariance matrix.

IV. SIMILARITIES BETWEEN DL MVDR BEAMFORMING AND FLOC MVDR BEAMFORMER

Diagonal loading (DL) is a classical and efficient approach to improve the robustness of the MVDR beamforming [1], [23]. In this section, we explore the similarities between the DL MVDR beamformer and the FLOC MVDR beamformer.

To begin with, we provide the expression of the WNAG of the DL MVDR beamformer G_{DL}. As a robust beamformer, the weight of the DL MVDR beamformer is obtained by [1]

$$\mathbf{w}_{\text{DL}} = \frac{(\mathbf{R}_{\mathbf{x}} + \sigma_{\text{DL}}^2 \mathbf{I})^{-1} \mathbf{a}_0}{\mathbf{a}_0^H (\mathbf{R}_{\mathbf{x}} + \sigma_{\text{DL}}^2 \mathbf{I})^{-1} \mathbf{a}_0}. \quad (31)$$

Then we get the explicit form of G_{DL} in the following corollary.

Corollary 1: Assume that σ_{DL}^2 is the amount of diagonal loading and $\lambda_1, \lambda_2, \cdots, \lambda_M$ are the eigenvalues of $\mathbf{R}_{\mathbf{x}}$. Let

$$\lambda_{\text{DL},k} = \lambda_k + \sigma_{\text{DL}}^2, \quad k = 1, 2, \ldots, M. \quad (32)$$

Then the WNAG of the DL MVDR beamformer is given by

$$G_{\text{DL}} = \frac{\left(t_1 \lambda_{\text{DL},1}^{-1} + t_2 \lambda_{\text{DL},2}^{-1} + \cdots + t_M \lambda_{\text{DL},M}^{-1}\right)^2}{t_1 \lambda_{\text{DL},1}^{-2} + t_2 \lambda_{\text{DL},2}^{-2} + \cdots + t_M \lambda_{\text{DL},M}^{-2}}, \quad (33)$$

where the constant t_i satisfies $0 \leq t_i < M$, $i = 1, 2, \cdots, M$, and $t_1 + t_2 + \cdots + t_M = M$.

Obviously, the expression of G_{DL} in (33) is similar to that of G in (23). In fact, the proof is analogous to that of Theorem 1 by using $\left(\mathbf{R}_{\mathbf{x}} + \sigma_{\text{DL}}^2 \mathbf{I}\right)$ instead of Ω. Hence, we omit the detail.

Moreover, we consider the eigenvalues of covariance matrix $\left(\mathbf{R}_{\mathbf{x}} + \sigma_{\text{DL}}^2 \mathbf{I}\right)$. By Definition 1, we have

$$\begin{aligned} &\text{Dis}\,(\lambda_{\text{DL},1}, \lambda_{\text{DL},2}, \cdots, \lambda_{\text{DL},M}) - \text{Dis}\,(\lambda_1, \lambda_2, \cdots, \lambda_M) \\ &= \sum_{j=1}^{M-1} \left(\frac{\lambda_{\text{DL},M}}{\lambda_{\text{DL},j}} - \frac{\lambda_M}{\lambda_j} \right) = \sum_{j=1}^{M-1} \frac{\sigma_{\text{DL}}^2 (\lambda_j - \lambda_M)}{(\lambda_j + \sigma_{\text{DL}}^2) \lambda_j}. \end{aligned} \quad (34)$$

Since $\lambda_j > \lambda_M > 0$ $(j = 1, 2, \ldots, M-1)$, (34) leads to

$$\text{Dis}\,(\lambda_{\text{DL},1}, \lambda_{\text{DL},2}, \cdots, \lambda_{\text{DL},M}) > \text{Dis}\,(\lambda_1, \lambda_2, \cdots, \lambda_M). \quad (35)$$

(35) indicates the eigenvalues of covariance matrix $\left(\mathbf{R}_{\mathbf{x}} + \sigma_{\text{DL}}^2 \mathbf{I}\right)$ separate less than those of covariance matrix $\mathbf{R}_{\mathbf{x}}$, which coincides with our result that the eigenvalue separation of FLOC based matrix is weaker than that of $\mathbf{R}_{\mathbf{x}}$.

Last, it has been proved that the WNAG of the DL MVDR beamformer is greater than that of the conventional MVDR
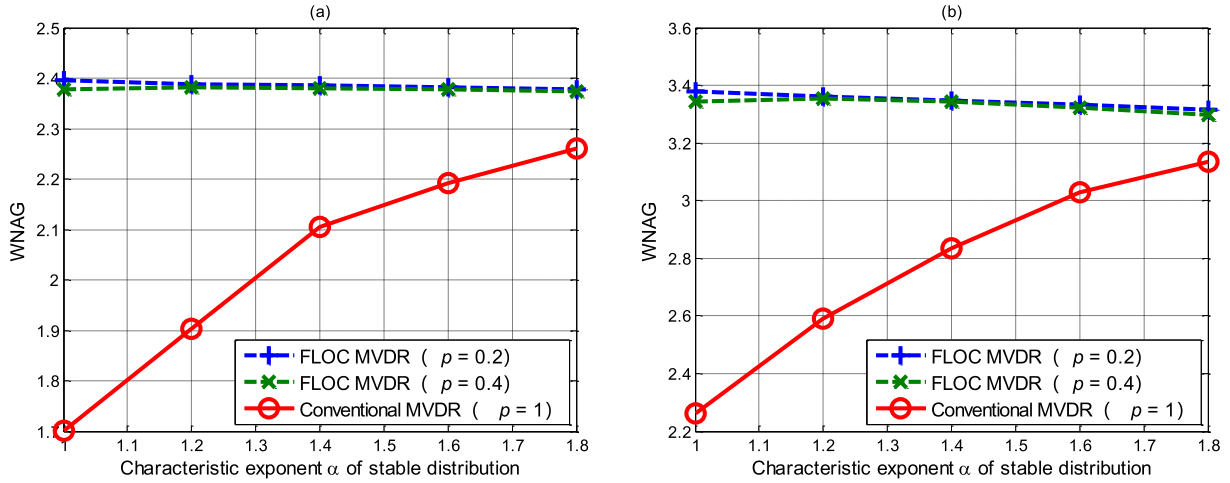
FIGURE 1. The WNAG comparisons between the FLOC MVDR beamformer and the conventional MVDR beamformer versus characteristic exponent α. (a) six-element array, (b) twelve-element array. The WNAGs of the FLOC MVDR beamformer are greater than those of the conventional MVDR beamformer under the FLOA($\alpha < 2$) noise.
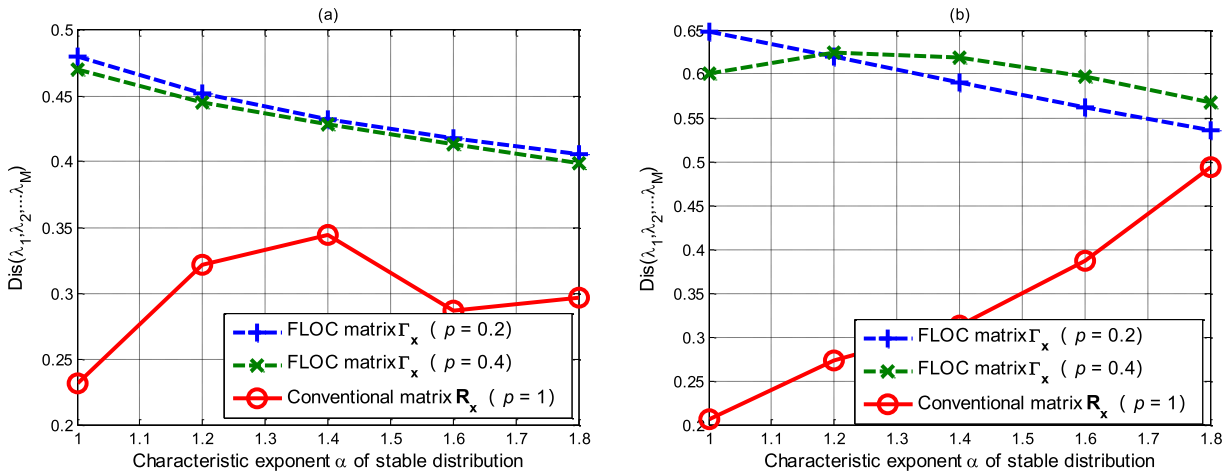
FIGURE 2. Eigenvalue separation Dis $(\lambda_1, \lambda_2, \cdots, \lambda_M)$ versus characteristic exponent α. (a) six-element array, (b) twelve-element array. Eigenvalue separation of FLOC matrix Γ_x is larger than that of conventional matrix R_x under the FLOA($\alpha < 2$) noise.

beamformer (e.g. [1]). Therefore, the DL MVDR beamformer and the FLOC MVDR beamformer also share the common property that both of their WNAGs are greater than the WNAG of the conventional MVDR beamformer.

Consequently, there are similarities in the expression, in the eigenvalue separation and in WNAG between the DL MVDR beamformer and the FLOC MVDR beamformer.

V. SIMULATIONS

This section consists of two parts. In the first part, we present the simulations to verify the analytical results of Section III. In the second part, we devote to investigate the performance of the FLOC MVDR beamformer when the received array noise obeys isotropic symmetric stable distributions.

A. SIMULATIONS FOR WNAG AND EIGENVALUE SEPARATION

The simulation settings in this subsection are as follows. We consider a uniform linear array with half wavelength element

spacing. The SOI arrives from 50° with $SNR_G = 0dB$ and two equal-power interferences arrive from $-40°$ and $0°$ with $INR_G = 0dB$. The length of snapshots is 1000. The WNAGs of the FLOC MVDR beamformer and the WNAGs of the conventional MVDR beamformer are plotted in Fig. 1 when the noise's characteristic exponent α changes from 1 to 1.8. All the curves in the figures are the average values of 200 independent simulations.

Figure 1 shows that the WNAGs of the FLOC MVDR beamformer are greater than those of the conventional MVDR beamformer in the presence of the FLOA noise. Under the same simulation settings, the Dis $(\lambda_1, \lambda_2, \cdots, \lambda_M)$ of Γ_x and that of R_x are illustrated in Fig. 2. We observe that Dis $(\lambda_1, \lambda_2, \cdots, \lambda_M)$ of Γ_x is larger than that of R_x when characteristic exponent $\alpha < 2$, which means that the eigenvalues of Γ_x separate less than those of R_x under the FLOA noise. Therefore, the reason that the WNAG of the FLOC MVDR beamformer, in the presence of the FLOA noise, is greater than that of the conventional MVDR beamformer

can be concluded that the eigenvalue separation of FLOC based matrix is weaker than that of conventional covariance.

B. PERFORMANCE OF FLOC MVDR BEAMFORMER

In this subsection, we investigate the performance of the FLOC MVDR beamformer in the presence of Gaussian ($\alpha = 2$) noise and the FLOA ($\alpha < 2$) noise, respectively. The array considered in this part is a uniform linear array of 6 isotropic elements with half wavelength element spacing. The look direction of the SOI is assumed to be 50°. There are two interferences which arrive from $-40°$ and $0°$. In all examples, we assume the SOI is always presented in the training data cell. We compare the performance of the FLOC MVDR beamformer against four alternative approaches including the MVDR beamformer [1], the MVDR-DL beamformer [23], the MVDR beamformer with forward-backward smoothing (MVDR-FB) [24] and the robust adaptive beamforming for general-rank signal models (BEAMFORMER-GR) [25].

The curves of optimal signal-to-interference-plus-noise ratio (SINR) [26]

$$\text{SINR}_{\text{opt}} = \sigma_s^2 \tilde{\mathbf{a}}_0^H \mathbf{R}_{i+n}^{-1} \tilde{\mathbf{a}}_0. \quad (36)$$

are included in Fig. 3, 5 and 7 as the benchmarks for Gaussian noise, while they are not inserted in Fig. 9, 11 and 13 since the optimal SINR (36) does not exist for the FLOA noise. Additionally, in Gaussian noise environment, the SINR is obtained by

$$\text{SINR} = \frac{\sigma_s^2 \left| \mathbf{w}^H \tilde{\mathbf{a}}_0 \right|^2}{\mathbf{w}^H \mathbf{R}_{i+n} \mathbf{w}}, \quad (37)$$

where σ_s^2 and $\tilde{\mathbf{a}}_0$ are the power and actual steer vector of SOI, respectively [26]. However, the SINR in (37) does not exist if the noise obeys the FLOA distribution. In this context, we define the geometric SINR

$$\text{SINR}_G = \frac{\exp \mathbb{E} \left[\ln \left(|s_0(k) \mathbf{w}^H \tilde{\mathbf{a}}_0| \right) \right]}{\exp \mathbb{E} \left[\ln \left(|\mathbf{w}^H \mathbf{x}_{i+n}(k)| \right) \right]} \quad (38)$$

to evaluate the SINR performance for the beamforming in the presence of the FLOA noise. As a result, the SNR, INR and SINR are calculated by the conventional definitions [1], [26] for Gaussian noise and by (4), (5) and (38) for the FLOA noise.

We test the performance of FLOC MVDR in following two parts. The first part consists of three examples which illustrate the performance in the presence of Gaussian noise. The other three examples are provided in the second part for the FLOA noise.

1) PERFORMANCE OF THE FLOC MVDR BEAMFORMER FOR GAUSSIAN NOISE

This part shows the performance of the beamformers in three scenarios with Gaussian noise. The INRs are fixed to be 10dB. The SNRs in Fig. 4, 6 and 8 are equal to 10dB. The diagonal loading factor of the MVDR-DL beamformer is $\sigma_{\text{DL}}^2 = 30$. Furthermore, we employ the constants $\gamma = 30$ and

$\varepsilon = 3$ for the BEAMFORMER-GR. All the weights of the beamformers are trained by 250 snapshots. The output SINR curves are the average values of 200 independent simulations.

Example 1: Exactly Known Signal Steering Vector.
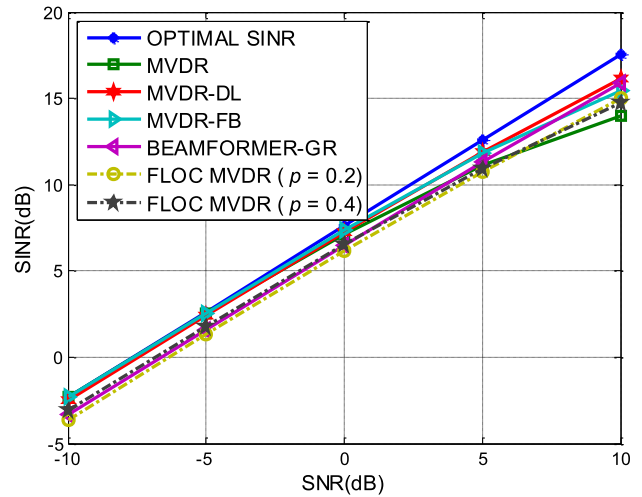
FIGURE 3. Comparison of the output SINR versus SNR. The signal steering vector is exactly known.

In Example 1, we simulate the scenario where the actual spatial signature of the signal is known exactly. Fig. 3 shows the output SINR versus SNR in this case. It is observed in Fig. 3 that the SINRs of the FLOC MVDR beamformer are comparable to those of the other four beamformers. The five beamformers have lower output SINRs than the optimal SINRs due to the presence of the signal of interest in the training data cell.
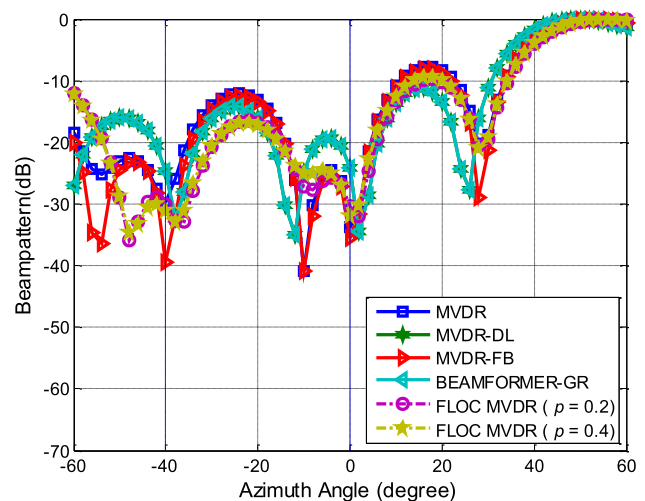
FIGURE 4. Comparison of the beampatterns. The signal steering vector is exactly known.

Fig. 4 plots the beampatterns of the five aforementioned beamformers. We observe that the MVDR beamformer and the FLOC MVDR beamformer cast deep nulls at the directions of interferences. Although the MVDR-FB beamformer

casts deeper nulls than the other algorithms, its null deviates from the true directions of interference with 2° shifting. Fig. 4 also indicates that the FLOC MVDR beamformers point their mainlobes towards the SOI direction at 50°.
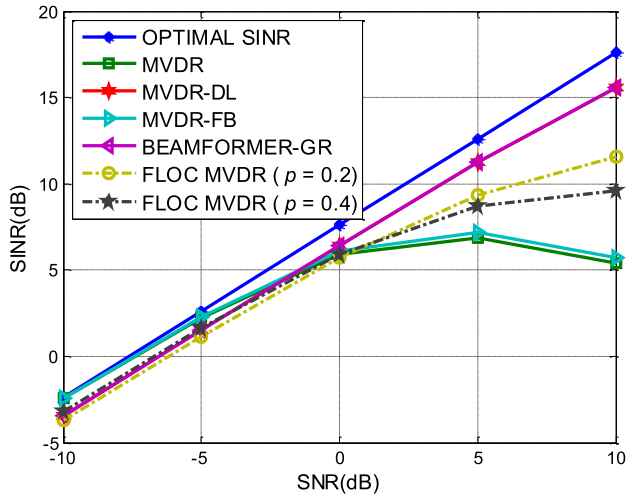
Example 2: Look Direction Mismatch

FIGURE 5. Output SINR versus SNR in the presence of look direction mismatches. The look direction error $\triangle\theta$ is assumed to be a Gaussian random variable with zero mean and standard deviation $\sqrt{3}°$.

Example 2 is concerned with the scenario in the presence of the signal look direction mismatches. The assumed SOI's look direction is 50° and the actual look direction is $50° + \triangle\theta$, where $\triangle\theta$ is the look direction error. Fig. 5 compares the output SINRs in the presence of the look direction error, where the look direction estimation error $\triangle\theta$ is a Gaussian random variable with zero mean and standard deviation $\sqrt{3}°$. This figure reveals that there has been obvious decrease in the SINRs of the MVDR beamformer when the SNRs are greater than 0dB. Surprisingly, the output SINRs of the FLOC MVDR beamformer are higher than those of the MVDR beamformer and the MVDR-FB beamformer.

Additionally, we present the beampatterns for the five beamformers in the scenario of the look direction error $\triangle\theta = 3°$ for Gaussian noise. It is observed from Figure 6 that both of the MVDR beamformer and the FLOC MVDR beamformer cast deep nulls in the interference directions. In the look direction, the MVDR beamformer casts a null about 10dB at 50°, which means the desired signal is suppressed. However, the FLOC MVDR beamformer casts a null about 5dB at 50°. These results suggest that the FLOC MVDR beamformer is more robust than the MVDR beamformer in the presence of look direction mismatches.

Example 3: Array Random Perturbation

Example 3 corresponds to the scenario of array random perturbations. Here the perturbation is modeled by a zero-mean Gaussian random variable with standard deviation σ_p. The perturbation steer vector of angle θ_j is given
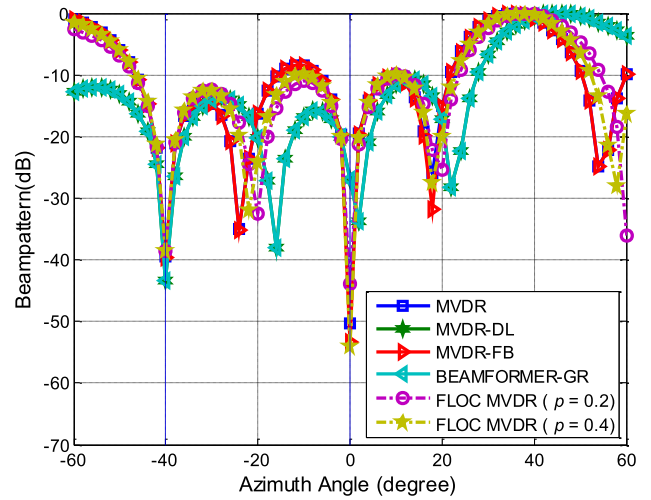

FIGURE 6. Beampatterns in the presence of the look direction error $\triangle\theta = 3°$.
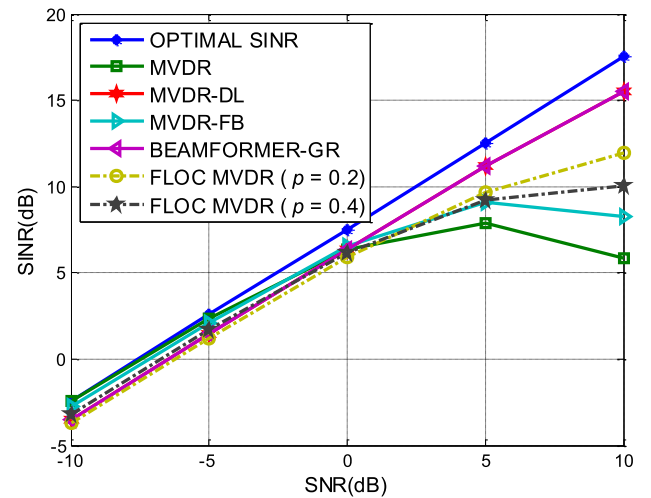

FIGURE 7. Output SINR versus SNR in the presence of array random perturbations. The random perturbation is assume to be a Gaussian random variable with zero mean and standard deviation $\sigma_p = 0.03\lambda$.

by [1]

$$a_p(\theta_j) = \left[1, \exp\left\{ i\frac{2\pi}{\lambda} d \sin(\theta_j) \left(1 + \Phi(\theta_j) \right) \right\}, \dots, \right.$$
$$\left. \exp\left\{ i\frac{2\pi}{\lambda} d \sin(\theta_j) \left(M - 1 + \Phi(\theta_j) \right) \right\} \right]^T, \quad (39)$$

where $\Phi(\theta_j) = \nu \sin\theta_j + \nu \cos\theta_j$ and ν is a Gaussian random variable with zero mean and standard deviation σ_p. We plot the output SINRs in the presence of array random perturbations with $\sigma_p = 0.03\lambda$ in Fig. 7. It is observed from the figure that the BEAMFORMER-GR yields higher output SINRs which are proportional to the SNRs. As the SNR increases, there exists SINR degradation for the MVDR beamformer caused by the look direction mismatches and the FLOC MVDR beamformer outperforms the MVDR beamformer.
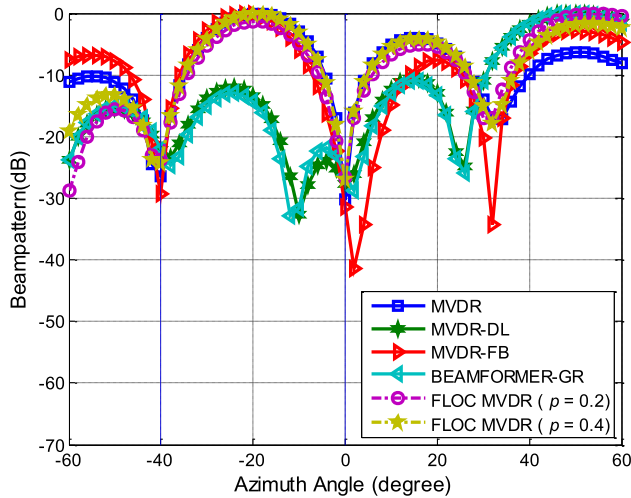
FIGURE 8. Beampatterns in the presence of the array perturbation. The amount of the perturbation is $v = 0.05$.

FIGURE 9. Output SINR$_G$ versus SNR$_G$ in the presence of the FLOA noise ($\alpha = 1.6$). The signal steering vector is exactly known.

Furthermore, we plot the beampatterns when the amount of the array perturbation is $v = 0.05$ in Fig. 8. It is seen that the MVDR beamformer and the FLOC MVDR beamformer cast deep nulls at the directions of interferences. However, at the look direction 50°, the FLOC MVDR beamformer maintains higher array gain than the MVDR beamformer.

2) PERFORMANCE OF THE FLOC MVDR BEAMFORMER FOR THE FLOA NOISE

In this part, we display the performance of the FLOC MVDR beamformer in the three scenarios which have been considered in the first part. Nevertheless, the received array noise is the FLOA noise with $\alpha = 1.6$ rather than Gaussian noise. The geometric INRs are fixed to be 10dB and the geometric SNRs in Fig. 10, 12 and 14 are equal to 10dB. The diagonal loading factor of the MVDR-DL beamformer is $\sigma_{DL}^2 = 100$. We employ the constants $\gamma = 100$ and $\varepsilon = 3$ for the BEAMFORMER-GR.

Example 4: In the Presence of FLOA Noise with Signal Steering Vector Known Exactly.

The purpose of Example 4 is to investigate the performance in the presence of the FLOA noise ($\alpha = 1.6$) without any steering vector error. We plot the output geometric SINRs versus SNR$_G$ in Fig. 9. As the SNR$_G$ increases, the MVDR beamformer shows performance degradation due to the presence of the SOI in the training data cell, while the FLOC MVDR beamformer achieves the highest output geometric SINRs among the five beamformers. We also plot the beampatterns in Fig. 10. Although all the beamformers cast nulls at the directions of interferences, the FLOC MVDR beamformer tends to have the lowest sidelobe level.

Example 5: In the Presence of Both the FLOA Noise and the Look Direction Mismatch

Example 5 corresponds to the performance of the FLOC MVDR beamformer in the presence of the look direction errors and the FLOA noise ($\alpha = 1.6$). Fig. 11 illustrates that
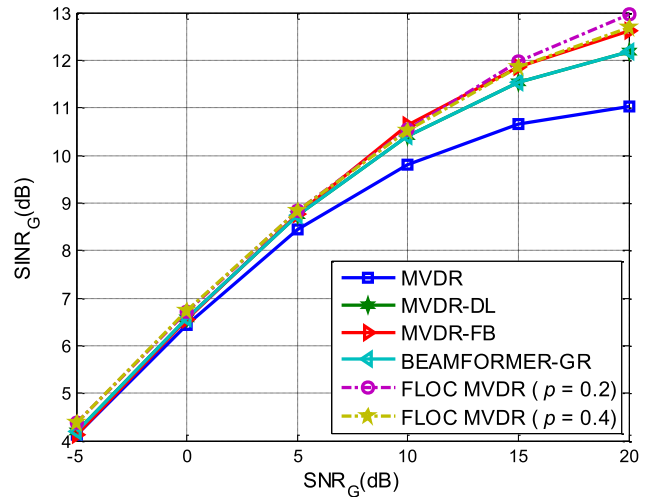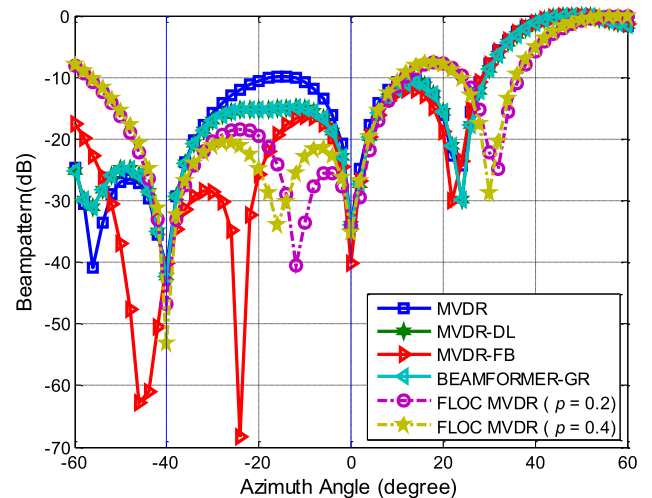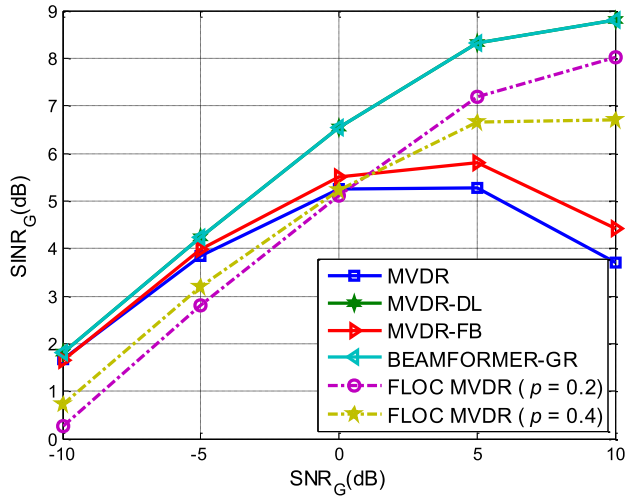

FIGURE 10. Beampatterns in the presence of the FLOA noise ($\alpha = 1.6$). The signal steering vector is exactly known.

the FLOC MVDR beamformer obtains the higher geometric SINRs than the MVDR beamformer when geometric SNRs are greater than 0dB. Moreover, the beampatterns are presented in Fig. 12 when the look direction error is $\triangle \theta = 3°$. Although the MVDR beamformer and the FLOC MVDR beamformer have the similar performance in suppressing the interferences, the former attenuates SOI about 10 dB whereas the latter improves the gain of the SOI about 5 dB.
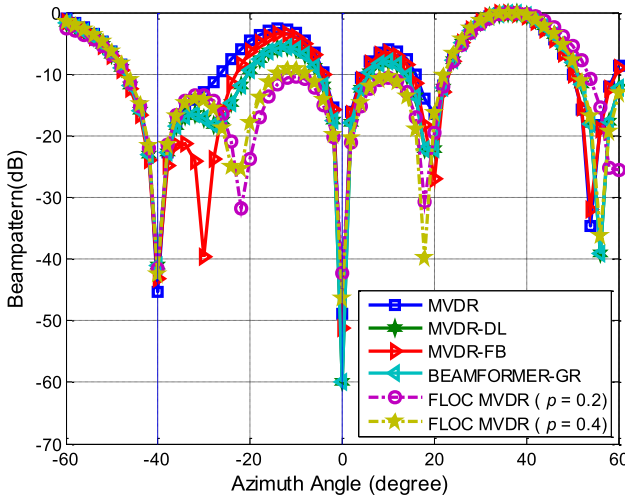
Example 6: In the Presence of Both the FLOA Noise and the Array Random Perturbation

The last example aims to examine the performance in the presence of both the FLOA noise and the array random perturbations. The settings of this example are the same as those of *Example 3* except that the received array noise is FLOA with $\alpha = 1.6$. The output geometric SINRs in Fig. 13 demonstrate that the FLOC MVDR beamformer outperforms the MVDR beamformer for higher geometric SNRs.
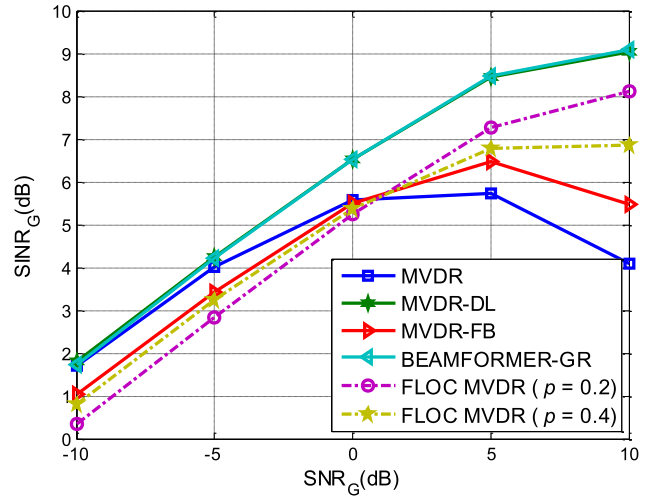
FIGURE 11. Output $SINR_G$ versus SNR_G in the presence of the FLOA noise ($\alpha = 1.6$) and look direction mismatches. The look direction error $\Delta\theta$ is assumed to be a Gaussian random variable with zero mean and standard deviation $\sqrt{3}°$.

FIGURE 13. Output $SINR_G$ versus SNR_G in the presence of the FLOA noise ($\alpha = 1.6$) and array random perturbations. The random perturbation is assume to be a Gaussian random variable with zero mean and standard deviation $\sigma_P = 0.03\lambda$.
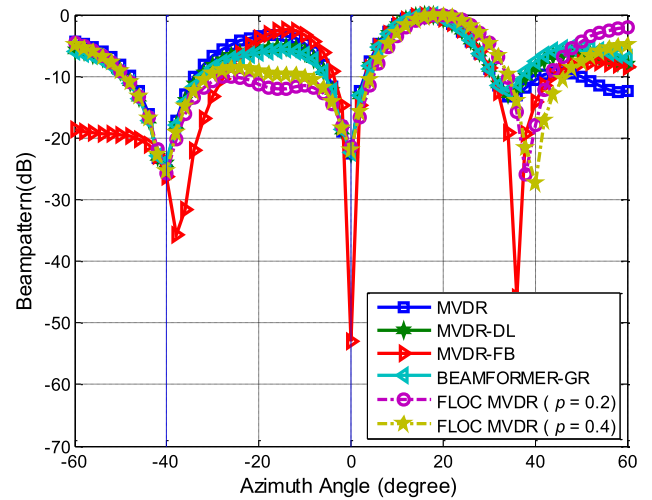

FIGURE 12. Beampatterns in the presence of the FLOA noise ($\alpha = 1.6$) and the look direction mismatch. The look direction error $\Delta\theta$ is fixed to be 3°.

FIGURE 14. Beampatterns in the presence of the FLOA noise ($\alpha = 1.6$) and the array perturbation. The amount of the perturbation is $v = 0.05$.

Furthermore, we show the beampatterns in Fig. 14. It is observed that the mainlobe of the FLOC MVDR beamformer is relatively higher than the MVDR beamformer. These results indicate that the FLOC MVDR beamformer provides more robustness than the MVDR beamformer in the presence of the FLOA noise and the array random perturbations.

In summary, these simulations show that the FLOC MVDR beamformer enjoys the best performance in the presence of the FLOA noise ($\alpha = 1.6$) without any steering vector error. When there exist steering vector mismatches, the MVDR-DL beamformer and the BEAMFORMER-GR outperform the FLOC MVDR beamformer due to adopting the suitable amount of diagonal loading. However, the FLOC MVDR beamformer is more robust than the MVDR beamformer against the steering vector mismatches for higher SNRs, which can be explained by the fact that the FLOC MVDR

beamformer's WNAG is greater than that of the conventional MVDR beamformer. Moreover, the figures in Subsection V-B show that the FLOC MVDR beamformer plays similar role to the MVDR-DL beamformer. A possible explanation for this might be that the MVDR-DL beamformer and the FLOC MVDR beamformer share the common property that both of their WNAGs are greater than that of the MVDR beamformer in the presence of the FLOA noise.

VI. CONCLUSIONS

In order to find out the reason why the WNAG of the FLOC MVDR beamformer is greater than that of the conventional MVDR beamformer under the FLOA noise, we first derive the explicit expression of WNAG, which is appropriate for both the FLOC MVDR beamformer and the conventional MVDR beamformer (Theorem 1). Then we analyze the

relationship between the WNAG and the eigenvalue separation by the expression of WNAG and conclude that the WNAG increases with the growth of the eigenvalue separation (Theorem 2), which results in the property that the WNAG of the FLOC MVDR beamformer is greater than that of the conventional MVDR beamformer. Moreover, we present the similarities in the expression, in the eigenvalue separation and in WNAG between the DL MVDR beamformer and the FLOC MVDR beamformer. The simulation results show that the FLOC MVDR beamformer, in the presence of the steer vector mismatches, offers improved performance compared to the MVDR beamformer when the received array noise obeys stable distributions.

APPENDIX A
PROOF OF THEOREM 1

According to the definition of WNAG in (19), the WNAG of either the conventional MVDR beamformer (10) or the FLOC MVDR beamformer (11) can be written as follows:

$$G = \frac{\left(\mathbf{a}_0^H \Omega^{-1} \mathbf{a}_0\right)^H \left(\mathbf{a}_0^H \Omega^{-1} \mathbf{a}_0\right)}{\mathbf{a}_0^H \Omega^{-2} \mathbf{a}_0}. \tag{40}$$

As Ω is Hermitian, there exists a unitary matrix $\mathbf{U}$ such that

$$\Omega = \mathbf{U}^H \Lambda \mathbf{U}, \tag{41}$$

where $\Lambda = diag(\lambda_1, \cdots, \lambda_M)$ and $\lambda_1, \cdots, \lambda_M$ are the real eigenvalues of Ω. Since Ω is positive semidefinite and nonsingular, we set $\lambda_1 \geq \lambda_2 \geq \cdots \geq \lambda_M > 0$ without loss of the generality. By (41), we get

$$\Omega^{-1} = \mathbf{U}^H \Lambda^{-1} \mathbf{U} \tag{42}$$

and

$$\left(\Omega^{-1}\right)^H \left(\Omega^{-1}\right) = \mathbf{U}^H \Lambda^{-2} \mathbf{U}, \tag{43}$$

where $\Lambda^{-1} = diag\left(\lambda_1^{-1}, \cdots, \lambda_M^{-1}\right)$. Substituting (42) and (43) in (40), we obtain

$$G = \frac{\left[(\mathbf{U}\mathbf{a}_0)^H \Lambda^{-1} (\mathbf{U}\mathbf{a}_0)\right]^H \left[(\mathbf{U}\mathbf{a}_0)^H \Lambda^{-1} (\mathbf{U}\mathbf{a}_0)\right]}{(\mathbf{U}\mathbf{a}_0)^H \Lambda^{-2} (\mathbf{U}\mathbf{a}_0)}. \tag{44}$$

Set

$$\mathbf{U}\mathbf{a}_0 = (c_1, c_2, \cdots, c_M). \tag{45}$$

Then (44) can be written as

$$G = \frac{\left(c_1^* c_1 \lambda_1^{-1} + c_2^* c_2 \lambda_2^{-1} + \cdots + c_M^* c_M \lambda_M^{-1}\right)^2}{c_1^* c_1 \lambda_1^{-2} + c_2^* c_2 \lambda_2^{-2} + \cdots + c_M^* c_M \lambda_M^{-2}}. \tag{46}$$

Let

$$t_1 = c_1^* c_1, \quad t_2 = c_2^* c_2, \quad \cdots, \quad t_M = c_M^* c_M. \tag{47}$$

Then we obtain (23). Moreover, from (47), we have

$$t_1 + t_2 + \cdots + t_M = (\mathbf{U}\mathbf{a}_0)^H (\mathbf{U}\mathbf{a}_0) = \mathbf{a}_0^H \mathbf{a}_0 = M \tag{48}$$

and $0 \leq t_i < M$, $i = 1, 2, \cdots, M$, which completes the proof.

APPENDIX B
PROOF OF THEOREM 2

Differentiating $G = h(u_1, u_2, \cdots, u_{M-1})$ with u_i, $i = 1, 2, \cdots, M - 1$, we have

$$\frac{\partial G}{\partial u_i} = \frac{\partial h(u_1, u_2, \cdots, u_{M-1})}{\partial u_i}$$

$$= \frac{2 t_i \left(\sum_{j=1}^{M-1} t_j u_j + t_M\right)}{\left(\sum_{j=1}^{M-1} t_j u_j^2 + t_M\right)^2} [t_M (1 - u_i)$$

$$+ \sum_{j=1, j \neq i}^{M-1} t_j u_j (u_j - u_i)]. \tag{49}$$

It follows from (47) and (27) that

$$\sum_{j=1}^{M-1} t_j u_j + t_M > 0.$$

Since $u_{M-1} \ll 1$, we get

$$\sum_{j=1, j \neq i}^{M-1} t_j u_j (u_j - u_i) + t_M (1 - u_i) > 0. \tag{50}$$

Substituting (50) in (49), we have (30).

REFERENCES

[1] L. V. T. Harry, *Optimum Array Processing (Detection, Estimation, and Modulation Theory, Part IV)*. New York, NY, USA: Wiley, 2002, pp. 1–664.

[2] Y. I. Abramovich, J. F. Gordon, and B. A. Johnson, "Iterative adaptive Kronecker MIMO radar beamformer: Description and convergence analysis," *IEEE Trans. Signal Process.*, vol. 58, no. 7, pp. 3681–3691, Jul. 2010.

[3] S. Zaidi and S. Affes, "Distributed collaborative beamforming in the presence of angular scattering," *IEEE Trans. Commun.*, vol. 62, no. 5, pp. 1668–1680, May 2014.

[4] S. Hur, T. Kim, D. J. Love, J. V. Krogmeier, T. A. Thomas, and A. Ghosh, "Millimeter wave beamforming for wireless backhaul and access in small cell networks," *IEEE Trans. Commun.*, vol. 61, no. 10, pp. 4391–4403, Oct. 2013.

[5] B. Bejar Haro, S. Zazo, and D. P. Palomar, "Energy efficient collaborative beamforming in wireless sensor networks," *IEEE Trans. Signal Process.*, vol. 62, no. 2, pp. 496–510, Jan. 2014.

[6] C. L. Nikias and M. Shao, *Signal Processing with Alpha-Stable Distributions and Applications*. New York, NY, USA: Wiley, 1995, pp. 1–140.

[7] Y. Liu, Z.-P. Huang, S.-J. Su, and C.-W. Liu, "AR model whitening and signal detection based on GLD algorithm in the non-Gaussian reverberation," *Appl. Acoust.*, vol. 73, no. 10, pp. 1045–1051, 2012.

[8] Y. Bian, "Polarimetric SAR statistical analysis using alpha-stable distribution and its application in optimal despeckling," *Int. J. Remote Sens.*, vol. 34, no. 19, pp. 6796–6836, Jun. 2013.

[9] G. Yu, C. Li, and J. Zhang, "A new statistical modeling and detection method for rolling element bearing faults based on alpha–stable distribution," *Mech. Syst. Signal Process.*, vol. 41, pp. 155–175, Dec. 2013.

[10] G. Sureka and K. Kiasaleh, "Sub-optimum receiver architecture for AWGN channel with symmetric alpha-stable interference," *IEEE Trans. Commun.*, vol. 61, no. 5, pp. 1926–1935, May 2013.

[11] X. Zhu, W.-P. Zhu, and B. Champagne, "Spectrum sensing based on fractional lower order moments for cognitive radios in α-stable distributed noise," *Signal Process.*, vol. 111, pp. 94–105, Jun. 2015.

[12] P. Tsakalides and C. L. Nikias, "Robust space-time adaptive processing (STAP) in non-Gaussian clutter environments," *IEE Proc. Radar, Sonar Navigat.*, vol. 146, no. 2, pp. 84–93, Apr. 1999.

[13] D.-F. Zha and T.-S. Qiu, "New beamforming method based on fractional lower order covariance matrix," *J. Commun.*, vol. 26, no. 7, pp. 16–20, 2005.

[14] J. He and Z. Liu, "Robust adaptive beamforming method in impulsive noise," *Chin. J. Electron.*, vol. 34, no. 3, pp. 464–468, 2006.

[15] J. He, Z. Liu, and K. T. Wong, "Linearly constrained minimum-'geometric power' adaptive beamforming using logarithmic moments of data containing heavy-tailed noise of unknown statistics," *IEEE Antennas Wireless Propag. Lett.*, vol. 6, pp. 600–603, 2007.

[16] J. He and Z. Liu, "Linearly constrained minimum-'normalised variance' beamforming against heavy-tailed impulsive noise of unknown statistics," *IET Radar Sonar Navigat.*, vol. 2, no. 6, pp. 449–457, Dec. 2008.

[17] H. Tang, T. Li, T. Qiu, and Y. Park, "Constant modulus algorithm for cochannel signal separation in non-Gaussian impulsive noise environments," *Wireless Pers. Commun.*, vol. 54, pp. 591–604, Sep. 2010.

[18] H. Tang, T. S. Qiu, and T. Li, "Capture properties of the generalized CMA in alpha-stable noise environment," *Wireless Pers. Commun.*, vol. 49, pp. 107–122, Apr. 2009.

[19] B. Liao and S. C. Chan, "Robust recursive beamforming in the presence of impulsive noise and steering vector mismatch," *J. Signal Process. Syst.*, vol. 73, no. 1, pp. 1–10, Oct. 2013.

[20] J. G. Gonzalez, J. L. Paredes, and G. R. Arce, "Zero-order statistics: A mathematical framework for the processing and characterization of very impulsive signals," *IEEE Trans. Signal Process.*, vol. 54, no. 10, pp. 3839–3851, Oct. 2006.

[21] A. B. Ramirez, G. R. Arce, D. Otero, J.-L. Paredes, and B. M. Sadler, "Reconstruction of sparse signals from ℓ_1 dimensionality-reduced Cauchy random projections," *IEEE Trans. Signal Process.*, vol. 60, no. 11, pp. 5725–5737, Nov. 2012.

[22] S. A. Vorobyov, "Principles of minimum variance robust adaptive beamforming design," *Signal Process.*, vol. 93, no. 12, pp. 3264–3277, 2013.

[23] B. D. Carlson, "Covariance matrix estimation errors and diagonal loading in adaptive arrays," *IEEE Trans. Aerosp. Electron. Syst.*, vol. 24, no. 4, pp. 397–401, Jul. 1988.

[24] K.-C. Huarng and C.-C. Teh, "Adaptive beamforming with conjugate symmetric weights," *IEEE Trans. Antennas Propag.*, vol. 39, no. 7, pp. 926–932, Jul. 1991.

[25] S. Shahbazpanahi, A. B. Gershman, Z.-Q. Luo, and K. M. Wong, "Robust adaptive beamforming for general-rank signal models," *IEEE Trans. Signal Process.*, vol. 51, no. 9, pp. 2257–2269, Sep. 2003.

[26] S. A. Vorobyov, A. B. Gershman, and Z.-Q. Luo, "Robust adaptive beamforming using worst-case performance optimization: A solution to the signal mismatch problem," *IEEE Trans. Signal Process.*, vol. 51, no. 2, pp. 313–324, Feb. 2003.
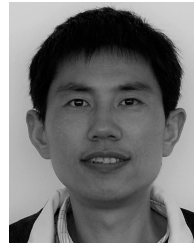
AIMIN SONG was born in 1978. He received the B.S. degree in mathematics from Liaoning Normal University, Dalian, in 2002, and the M.S. degree in mathematics and the Ph.D. degree in electronic and information engineering from the Dalian University of Technology, Dalian, in 2005 and 2015, respectively. He is currently a Lecturer from the School of Science, Dalian Jiaotong University, China. His current research interests include time delay estimation, adaptive beamforming, and stochastic control.

● ● ●